

# MR temperature imaging using PRF phase difference and a geometric model-based fat suppression method

Shoubin Liu\* and Yanming Zhou

*Department of Mechanical Engineering and Automation, Harbin Institute of Technology Shenzhen Graduate School, Shenzhen University Town, Xili, Shenzhen, China*

## Abstract.

**BACKGROUND:** Because protons in fat do not exhibit a temperature-dependent frequency shift, proton resonance frequency shift (PRFS)-based MR thermometry always suffers from disturbances due to the presence of fats or lipids.

**OBJECTIVE:** A new fat suppression method for PRFS-based MR thermometry is proposed to obtain accurate variation of phase angle.

**METHODS:** Similar to the approach of separating fat and water with the two-point Dixon technique, we first scan a complex MR image for reference and then scan another complex image varying with temperature at the same  $TE$  point. Based on the conventional PRFS method, we use geometric relationships to remove the effect of fat on the variation of the phase angle.

**RESULTS:** Two phantoms with different water-to-fat ratios are involved in the temperature mapping test. Experimental results show that the temperature images of two phantoms are approximated under the same conditions.

**CONCLUSIONS:** The proposed fat suppression method is simple and effective for PRFS-based MR thermometry.

Keywords: MR thermometry, PRFS, fat suppression, geometric model

## 1. Introduction

MRI not only offers soft tissue images with excellent contrast, but is also used for noninvasive temperature measurement. In addition, people are able to undergo a long scanning process without side effects, because MRI does not use radiation. These merits indicate that MRI has great potential for image-guided thermal therapy. One can obtain soft tissue and temperature images at the same time during a hyperthermic procedure. Parameters including the spin-lattice relaxation time  $T_1$ , the diffusion coefficient  $D$ , and the proton resonance frequency (PRF) of tissue water, are temperature sensitive and can be utilized for MR temperature mapping [1]. Among various methods of temperature mapping, the most promising one is proton resonance frequency shift (PRFS)-based MR thermometry. The PRFS-based techniques exploit the temperature dependence of the proton resonance frequency of water. A temperature change  $\Delta T$  will cause a change  $\sigma$  in the electron screening constant of the water protons. The ratio coefficient

---

\*Corresponding author: Shoubin Liu, Department of Mechanical Engineering and Automation, Harbin Institute of Technology Shenzhen Graduate School, Shenzhen University Town, Xili, Shenzhen, China. Tel.: +86 755 2603 3516; Fax: +86 755 2603 3774; E-mail: mesbliu@hitsz.edu.cn.

can be expressed as  $d\sigma_{wat}/dT = 0.01 \text{ ppm}/^\circ\text{C}$  [2]. However, conventional PRFS-based MR thermometry is negatively impacted by disturbances due to fat protons, motion-induced errors, and field drifts. With improvements in hardware equipment, optimizing the high-speed sequence, and using the compressed sensing (CS) algorithm [3], there have been noticeable changes in the effects of motion artifacts and magnetic field shifts. However, the problems that come with the presence of fat protons have not been perfectly resolved. PRFS-based techniques usually need a fat suppression process, which not only increases the imaging time but also leads to incomplete results due to amplitude inhomogeneities of the static field across a sample. Some researchers use generalized Dixon chemical shift-based water-fat separation methods to remove the effect of fat. Yet, this method is expected to fail as the voxel water-fat ratio approaches 100% or 0% [4]. In this paper, we propose a geometric model-based fat suppression method. We first capture two complex MR images from double scans at the same  $TE$  point, then make use of certain geometric relationships to remove the effect of fat and obtain the variation of the phase angle. Finally, we exploit the temperature sensitivity of tissue water protons to obtain relative temperature maps. The proposed MR thermometry method, called as the G-PRFS method, is not sensitive to inhomogeneities of magnetic field, and can significantly reduce the effect of fat. By characterizing inhomogeneities of the magnetic field using a field map, we can get a more accurate temperature map through independent manipulation of each pixel. Setting a reasonable threshold, the G-PRFS method degenerates into the conventional PRFS method as the voxel fat-water ratio approaches 0%. The G-PRFS method performs well when the fat content is relatively high. Because of the limitation of PRFS-based techniques, the G-PRFS method is also expected to fail as the voxel fat-water ratio approaches 100%.

## 2. Methods

When we neglect the influence of fat protons, the conventional PRFS method measures the temperature as follows.

Assuming that when collecting a single image, both the temperature change and inhomogeneities in each voxel can be neglected, the water proton resonant frequency can be expressed as:

$$\omega_{wat} = \gamma(1 + \sigma_0 + \sigma_T)B_0 \quad (1)$$

$$\sigma_T = \alpha\Delta T \quad (2)$$

where  $\sigma_T$  and  $\sigma_0$  represent the local magnetic field changes caused by temperature and non-temperature factors.  $\gamma$  is the gyro-magnetic ratio.  $B_0$  is the static magnetic field intensity.  $\Delta T$  is the temperature change between gradient-echo scans.  $\alpha$  is the temperature-dependent coefficient of the water proton chemical shift, which is about  $0.01 \text{ ppm}/^\circ\text{C}$ . To remove the effect of  $\sigma_0$ , we first acquire a complex image for reference, and then obtain another complex image. By subtracting the reference image, we obtain the phase image caused by the temperature. Therefore, as compared with the reference image, the variation of the angular frequency caused by the temperature can be written as:

$$\Delta\omega = \gamma\sigma_TB_0 \quad (3)$$

As shown in Fig. 1, the phase variation accumulated within  $TE$  is calculated by:

$$\Delta\Phi = \Delta\omega TE = \gamma\sigma_TB_0 TE = \gamma\alpha\Delta TB_0 TE \quad (4)$$

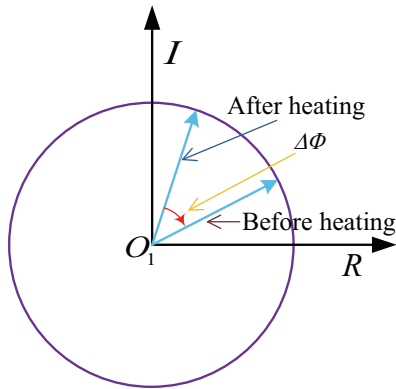


Fig. 1.  $\Delta\Phi$  is the phase variation entirely caused by the temperature change.

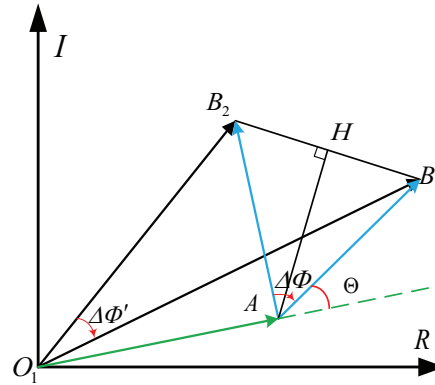


Fig. 2.  $\Delta\Phi$  and  $\Delta\Phi'$  are the temperature-dependent phase variation identified by the G-PRFS method and the conventional PRFS method.

Thus, the temperature change or the relative temperature is obtained by:

$$\Delta T = T - T_{ref} = \frac{\Delta\Phi}{\gamma\alpha B_0 TE} \tag{5}$$

In this approach, we ignore the influence of fat protons. In fact, fat protons are not sensitive to the temperature change, which causes errors in temperature measurement. When considering the influence of fat protons, we propose the G-PRFS method, which performs the temperature measurement as follows.

The complex signals in a voxel can be expressed as:

$$S(TE_i) = (W \cdot e^{j\Phi(T)} + F \cdot e^{j\Theta}) \cdot e^{j2\pi\Psi TE_i} \cdot e^{-R_2^* TE_i} \tag{6}$$

where  $W$  and  $F$  represent the water and the fat components in this voxel, respectively.  $\Phi(T)$  is the phase variation of water protons caused by the temperature.  $\Theta$  ( $\Theta = j2\pi\Delta f TE_j$ ,  $\Delta f = 220$  Hz at 1.5 T) denotes the frequency difference due to chemical shifts between the water and the fat [4].  $\Psi$  denotes the  $B_0$  field inhomogeneity at this voxel.  $R_2^*$  is the spin-spin relaxation rate ( $R_2^* = 1/T_2^*$ ). The signal in the voxel is composed of a complex water signal and a complex fat signal.

It is assumed that the amplitudes of the water and fat remain constant if there is change in temperature of less than 6°C. Figure 2 illustrates various complex signals of the G-PRFS method in the case of 1:1 water-to-fat ratio.

In Fig. 2,  $O_1B_1$  represents the reference signal.  $O_1B_2$  represents the signal after heating.  $O_1A$  represents the fat signal.  $AB_1$  denotes the reference water signal.  $AB_2$  is the water signal after heating.  $HA$  is the perpendicular bisector of  $B_1B_2$ .

When the voxel fat-water ratio approaches 0%, the G-PRFS method has the same effect as the conventional PRFS method. We then set a reasonable threshold that can increase the numerical stability of MR thermometry. The G-PRFS method adopts a double-gradient-echo sequence. The first echo image is acquired for temperature measurement. The rate of the corresponding pixel modulus values from the first echo and the second echo is used to measure the fat content. We define the threshold value by  $\lambda = O_1B'_1/O_1B_1$ , where  $O_1B_1$  and  $O_1B'_1$  from the first echo and the second echo represent the signal modulus values in the corresponding pixel. G-PRFS degenerates into the conventional PRFS method as  $\varepsilon < \lambda$ . The value of  $\varepsilon$  is determined by  $\Delta TE$  and  $T_2^{*}$ .

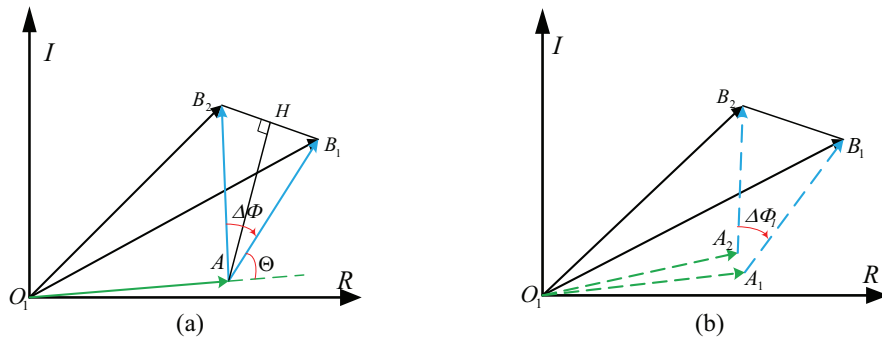


Fig. 3. (a) The G-PRFS method exploiting the complex images from the twice scans as  $TE = 22.80$  ms. (b) The complex water signal and the complex fat signal from five-point Dixon fat-water separation.

To verify the effectiveness of the G-PRFS method in a real situation, complex images were acquired with a BASDA 1.5 T machine. Three water-fat phantoms consisting of peanut-oil-in-gelatin dispersions were also produced [5]. The phantoms' water-to-fat ratio is 50:50 by volume. Five gradient echo images were acquired at each time for exploiting the five-point Dixon fat-water separation method [4]. The sequence parameters are  $TR = 45$  ms,  $TE = [16.67, 19.73, 22.80, 25.87, 28.94]$  ms,  $FOV = 25$  cm, scan matrix =  $256 \times 256$ ,  $BW = \pm 31.3$  kHz, slice thickness = 5 mm, averages = 2,  $B_0 = 1.5$  T. The temperature change between the two scans is  $6^\circ\text{C}$ . Figure 3 illustrates a comparison of the complex signals from the G-PRFS method and the five-point Dixon fat-water separation method.

The angle difference between  $\Delta\Phi'$  and  $\Delta\Phi_1$  is  $16^\circ$ , giving us a temperature difference of  $3.09^\circ\text{C}$ . The angle difference between  $\Delta\Phi$  and  $\Delta\Phi_1$  is  $1.5^\circ$ , which leads to a temperature difference of  $0.29^\circ\text{C}$ . As a result, the G-PRFS method is superior to the conventional PRFS method; the temperature error is small and within an acceptable range.

There is the temperature dependency of the proton density (about  $0.29\%/^\circ\text{C}$  [6]), which influences the amplitudes of fat and water signals. Fat protons are not entirely unaffected by changes in temperature. They have a temperature dependency of approximately  $0.00018$  ppm/ $^\circ\text{C}$  [7], which influences the chemical shift between water and fat signals and causes temperature errors in the G-PRFS method.

### 3. Results

In our experimental scheme, the sequence parameters are  $TR = 45$  ms,  $TE = 23$  ms,  $FOV = 25$  cm, scan matrix =  $256 \times 256$ ,  $BW = \pm 31.3$  kHz,  $FA = 25^\circ$ , slice thickness = 5 mm, averages = 2,  $B_0 = 1.5$  T. The phantoms' water-to-fat ratios are 40:60 and 60:40 by volume. We adopted an active heating approach [4]. The temperature changes smoothly during the experimental process.

We put phantoms into MR machine, and captured the reference image after the MR machine stabilized. Heating was begun, and it was noticed that the temperature of the phantoms increased smoothly. The relative temperature curve is recorded with a temperature sensor, as shown in Fig. 4(a). Three images are captured at 5 min time intervals. The first and second images are captured as the temperature increases, while the third image is obtained when the temperature is constant.

As shown in Fig. 4(b), column 1 represents the phantoms' relative temperature images at time point "1", where the reference temperature is that of the reference image captured. Column 2 and 3 represent phantoms' relative temperature images at time points "2" and "3". To calculate the relative temperature of a given pixel of a phantom, we adopt the complex signal  $O_1 B_2$  at time points "1", "2", or "3", and

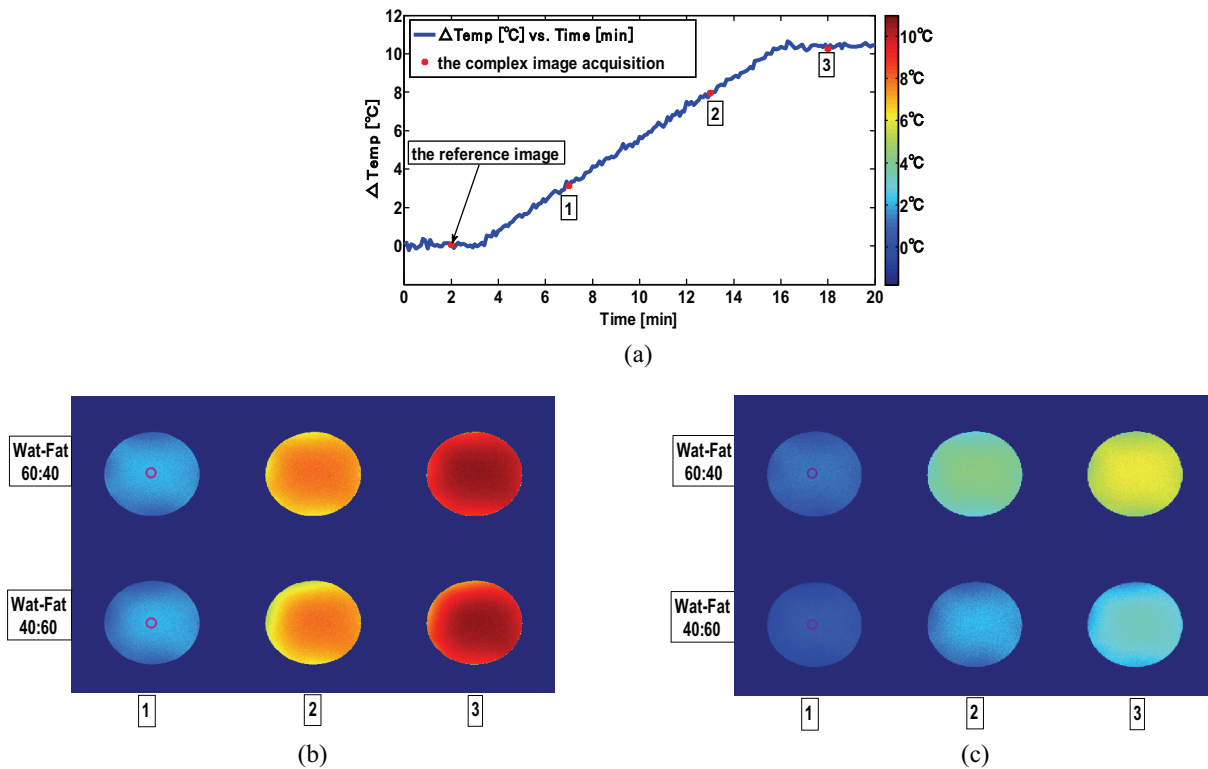


Fig. 4. The G-PRFS-based MR thermometry and the conventional PRFS-based MR thermometry for phantoms with different water-fat ratios: (a) Phantoms' relative temperature curve recorded by a temperature sensor. The reference time point is for acquisition of a reference image. Three time points "1", "2" and "3" are for acquisition of complex images at three different temperatures. (b) Measured relative temperature maps of two phantoms at three time points using the G-PRFS method. The small circles in column 1 indicate the location of temperature measured. (c) Measured relative temperature maps of two phantoms at three time points using the conventional PRFS method.

the complex signal  $O_1 B_1$  at the reference time point. Based on a geometric model, as shown in Fig. 2, we obtain the variation of the phase angle  $\Delta\Phi$ .  $\Delta T$  of the given pixel is further derived with Formula (5).

Figure 4(b) indicates that the relative temperature images of two phantoms with different water-to-fat ratios are approximated under the same conditions. This verifies that the G-PRFS-based MR thermometry method is unaffected by the water-to-fat ratio.

As a contrast, Fig. 4(c) illustrates two phantoms' relative temperature images at time points "1", "2" and "3" using the conventional PRFS method. It indicates that the relative temperature images of two phantoms are different under the same conditions. The different values are similar to the errors shown in literature [8].

#### 4. Conclusions

A new method regarding the G-PRFS method is proposed for MR thermometry. The G-PRFS method adopts a geometric model-based fat suppression method to reduce the effect of fat. The aim of this method is to obtain accurate variation of phase angle based on geometric relationships. The G-PRFS method is superior to the conventional PRFS method. The experimental results show that this method is simple and can significantly reduce the effect of fat.

MR temperature measurement has become an attractive method for tumor thermotherapy [9]. In the measurement of the temperature of the human body, the previous threshold can ensure the accuracy of temperature measurement as the voxel fat-water ratio approaches 0%. The  $TE$  can be optimized to improve the numerical stability of the MR thermometry and to maximize the signal-to-noise ratio (SNR) of the temperature maps [10]. When the  $TE$  is fixed, temperature changes should be small between the two scans to avoid the variation of the phase angle exceeding  $360^\circ$ . In addition, the G-PRFS method also suffers from some disturbances, including motion-induced errors and field drifts due to the need for a reference image.

## References

- [1] Rieke V, Pauly KB. MR Thermometry. *J. Magn. Reson. Imag.* 2008; 27: 376.
- [2] Hindman JC. Proton resonance shift of water in the gas and liquid states. *J. Chem. Phys.* 1966; 44: 4582.
- [3] Lustig M, Donoho D, Pauly JM. Sparse MRI: The application of compressed sensing for rapid MR imaging. *Magn. Reson. Med.* 2007; 58: 1182.
- [4] Soher BJ, Wyatt C, Reeder SB, MacFall JR. Noninvasive temperature mapping with MRI using chemical shift water-fat separation. *Magn. Reson. Med.* 2010; 63: 1238.
- [5] Madsen EL, Hobson MA, Frank GR, Shi H, Jiang J, Hall TJ, Varghese T, Dooley MM, Weaver JB. Anthropomorphic breast phantoms for testing elastography systems. *Ultrasound in Med. & Biol.* 2006; 32(6): 857.
- [6] Chen J, Daniel BL, Pauly KB. Investigation of proton density for measuring tissue temperature. *J. Magn. Reson. Imag.* 2006; 23: 430.
- [7] Stollberger R, Ascher PW, Huber D, Renhart W, Radner H, Ebner F. Temperature monitoring of interstitial thermal tissue coagulation using MR phase images. *J. Magn. Reson. Imag.* 1998; 8: 188.
- [8] Rieke V, Pauly KB. Echo combination to reduce proton resonance frequency (PRF) thermometry errors from fat. *J. Magn. Reson. Imag.* 2008; 27: 673.
- [9] Hynynen K. MRI-guided focused ultrasound treatments. *Ultrasonics* 2010; 50: 221.
- [10] De Zwart JA, Van Gelderen P, Kelly DJ, Moonen CTW. Fast magnetic resonance temperature imaging. *J. Magn. Reson. B.* 1996; 112: 86.